IEEE Access
Multidisciplinary | Rapid Review | Open Access Journal

Date of publication xxxx 00, 0000, date of current version xxxx 00, 0000.

Digital Object Identifier 10.1109/ACCESS.2017.DOI

Dependability of Directional Millimeter Wave Vehicle-to-Infrastructure Communications

STEFAN SCHWARZ[1], (Senior Member, IEEE), ERICH ZÖCHMANN[1], (Member, IEEE), MARTIN MÜLLER[1], (Member, IEEE) and KE GUAN[2], (Senior Member, IEEE)

[1]Christian Doppler Laboratory for Dependable Wireless Connectivity for the Society in Motion, Institute of Telecommunications, Technische Universität (TU) Wien, 1040 Vienna, Austria (e-mail: sschwarz@nt.tuwien.ac.at)

[2]State Key Laboratory of Rail Traffic Control and Safety, Beijing Engineering Research Center of High-speed Railway Broadband Mobile Communications, Beijing Jiaotong University, 100044 Beijing, China (e-mail: kguan@bjtu.edu.cn)

Corresponding author: S. Schwarz (e-mail: sschwarz@nt.tuwien.ac.at).

This work was supported by the Austrian Federal Ministry for Digital and Economic Affairs and the Austrian National Foundation for Research, Technology and Development.

ABSTRACT Vehicle-to-infrastructure (V2I) communication is an important enabler for intelligent transportation and rail traffic management systems, which are expected to provide significant road traffic safety and efficiency enhancements. Such systems require a level of dependability of the wireless communication link that can be hard to support by state-of-the-art technologies. Transmissions in the millimeter wave (mmWave) band have the potential to provide sufficient bandwidth to support not only traffic management services, but additionally also web and entertainment applications for car and train passengers. mmWave transmissions require directional antennas at the transmitter and/or receiver to compensate for the significant pathloss and to achieve a practically acceptable maximum coupling loss. Such directional communication is feasible in V2I scenarios, because the mobility of users is confined to streets and roads. In this article, we discuss the dependability of directional mmWave V2I communications under two-ray fading conditions. We review methods for enhancing the dependability of the communication link by exploiting macroscopic spatial diversity and by mitigating interference from other transmitters. We furthermore provide guidelines for a dependable system design under two-ray fading and identify open research questions in this context.

INDEX TERMS Dependability, directional antennas, two-wave with diffuse power fading channels, vehicular communications

I. INTRODUCTION

Vehicle-to-everything (V2X) communication is one of the main drivers of the development of 5G and beyond wireless communication technologies [1], [2]. Relevant V2X communication scenarios include traffic safety and efficiency related information exchange amongst vehicles and with infrastructure nodes along roads, as well as, efficient provisioning of web and entertainment services to passengers of cars and trains [3]. The field of safety related information exchange poses significant challenges for V2X communications, since it often requires a level of dependability, in terms of latency and reliability of data packet exchange, that is hard to support by state-of-the-art wireless communication technologies especially in crowded situations [4].

The basis of any optimal transceiver design is a channel model that accurately represents realistic channel conditions of the respective propagation environment. Recently, directional channel models gained significant interest in the contexts of full-dimension multiple-input multiple-output (FD-MIMO) transmission and three-dimensional (3D) beamforming, as well as, hybrid precoding architectures for millimeter wave (mmWave) systems [5], [6]. For vehicle-to-infrastructure (V2I) communication scenarios, directional channel models are also frequently adopted [7]–[9]. In this case, a direct line-of-sight (LOS) between transmitters and receivers is often guaranteed by proper placement of infrastructure nodes and road-side units (RSUs).

Many sophisticated methods for directional channel modeling exist. In mobile communications, often so called geometry-based stochastic channel models are employed [10], [11], e.g., the 3GPP 3D channel model speci-

This article has been accepted for publication in a future issue of this journal, but has not been fully edited. Content may change prior to final publication. Citation information: DOI 10.1109/ACCESS.2020.2981166, IEEE Access

fied in TR 36.873 and its 5G extension towards mmWaves in TR 38.901 [12], [13]. Such channel models are well-suited for generating random realizations of commonly encountered propagation environments, e.g., for rural/urban outdoor/indoor scenarios. If, on the other hand, a specific propagation geometry is given, ray-tracing methods are better suited for channel modeling [14], [15]. Both approaches, however, suffer from relatively high computational complexity and often lack the possibility to gain intuitive, let alone analytic insights into the performance of a communication system. Hence, even though these types of channel models are well suited for a realistic performance investigation of given transceiver architectures, they are hardly appropriate for deriving general guidelines that are useful for the basic transceiver design.

In this article, we argue that the most relevant fading characteristics of directional mmWave V2I communications can often be captured by relatively simple two-path (or two-ray) channel models, which still exhibit a certain level of analytical tractability. More specifically, the two-wave with diffuse power (TWDP) channel model has successfully been applied in a number of recent publications to model V2I channel measurement data and results from ray-tracing simulations in the mmWave band [16]–[18]. TWDP fading is known for its potentially worse-than-Rayleigh fading behavior in terms of signal outage probability [19], [23]. We therefore investigate how TWDP fading impacts the dependability of V2I communications. Based on the developed insights, we then discuss approaches to enhance the reliability of directional mmWave V2I communications by exploiting spatial diversity and by coordinating transmissions, and we provide guidelines for a dependable system design. Furthermore, we identify open research questions that arise when considering TWDP fading channels for intended and interfering signals.

II. TWO-PATH CHANNEL MODELS IN DIRECTIONAL MMWAVE COMMUNICATIONS

The focus of this article is on directional mmWave V2I communications, where either both the transmitter and the receiver, or at least one of them is equipped with a highly directional antenna to compensate for the significant pathloss encountered in mmWave transmissions [20]. An exemplary V2I communication scenario is illustrated in Fig. 1, where a train is served by RSUs along the railroad track.

In general, the directional multi-path propagation environment can be described by a channel impulse response of the form [21]

$$h(\tau) = \sum_{p=1}^{N} \alpha_p e^{j\varphi_p} g_t(\mathbf{\Psi}_{p,t}) g_r(\mathbf{\Psi}_{p,r}) \delta(\tau - \tau_p). \quad (1)$$

Here, α_p is the gain of the p-th path, φ_p is its phase-shift and τ_p is its delay. The functions $g_t(\mathbf{\Psi})$ and $g_r(\mathbf{\Psi})$ are the antenna gain patterns of the transmitter and the receiver and $\mathbf{\Psi}_{p,t} = (\phi_{p,t}, \theta_{p,t})$, $\mathbf{\Psi}_{p,r} = (\phi_{p,r}, \theta_{p,r})$ are the angles of departure and arrival, respectively. Although not explicitly shown, all of these parameters in general vary over time due to movement of the transmitters, receivers and/or scatterers.

The signal propagation in V2I scenarios such as illustrated in Fig. 1 can often be very well approximated by a much simpler two-path or two-ray fading channel model for the reasons summarized in the following two paragraphs.

A. SPATIAL FILTERING OF THE MULTI-PATH PROPAGATION ENVIRONMENT

In mmWave transmissions, highly directional antennas are necessary to compensate for the propagation pathloss, implying that the antenna gain patterns $g_t(\mathbf{\Psi})$ and $g_r(\mathbf{\Psi})$ are relatively sharp, e.g., with a 3 dB opening angle in the order of 10°. This especially applies for the considered V2I scenario, where the distances between transmitters and receivers can be large, and therefore large antenna gains are required. Such antennas act as spatial filters that effectively limit the richness of the multi-path propagation environment to few paths that align with the main lobe of the antenna. We thus approximate the channel impulse response as

$$h(\tau) \approx \sum_{p=1}^{M} \alpha_p e^{j\varphi_p} g_t(\mathbf{\Psi}_{p,t}) g_r(\mathbf{\Psi}_{p,r}) \delta(\tau - \tau_p), \quad (2)$$

where $M \ll N$ is the number of paths that "survive" this spatial filtering process.

How many paths M need to be considered depends on the propagation environment. The evidence reported in Section II-D suggests that in many V2I cases two paths are indeed sufficient to characterize the fading of the effective directional channel. The main reason for this behavior is that, in contrast to indoor environments, the distances to scattering objects are relatively large and therefore their contribution to the signal propagation becomes negligible if they fall outside the main lobe of the antenna. Furthermore, within the main lobe only few significant scattering objects are visible. We will therefore consider $M = 2$ below. Notice that this assumption will ultimately lead to TWDP fading of the effective channel. Since TWDP fading is known to represent the worst case in terms of outage behavior, this assumption is therefore well justified when investigating the dependability of a communication system.

B. TEMPORAL RESOLVABILITY OF PATHS

We argued above that the transmit and receive antennas act as spatial filters that limit the effective angular spread of the signal propagation to several degrees in the angular domain. This, however, also implies that the delay spread of the signal propagation will be significantly reduced [22].

For example, if we assume that the signal propagation is dominated by a direct LOS path and a ground surface reflection as illustrated in Fig. 1, the temporal difference between the direct path and the reflected path at horizontal distance

This article has been accepted for publication in a future issue of this journal, but has not been fully edited. Content may change prior to final publication. Citation information: DOI 10.1109/ACCESS.2020.2981166, IEEE Access

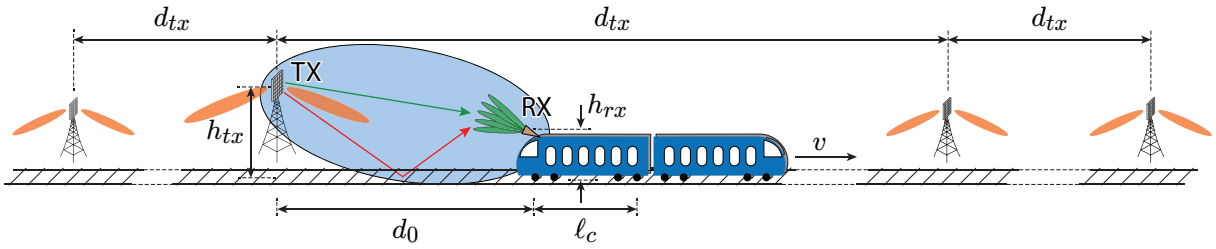

FIGURE 1. Illustration of a directional mmWave V2I communication scenario as considered in this paper. Both, the transmitter and receiver, are equipped with directional antennas, which effectively act as spatial filters for the multi-path propagation environment. The receive antenna on the train is considered to be steerable to enable alignment of the beam along the LOS direction.

d_0 between transmitter and receiver is approximately given by (assuming $d_0 \gg h_{tx}, h_{rx}$)

$$\Delta\tau \approx \frac{2h_{tx}h_{rx}}{d_0 c_0}, \tag{3}$$

where c_0 is the speed of light. In a representative railroad communication scenario with transmitter height $h_{tx} = 10\,\text{m}$, receiver height $h_{rx} = 3.5\,\text{m}$ and distance $d_0 = 100\,\text{m}$, the propagation delay difference equates to $\Delta\tau \approx 2.3\,\text{ns}$. This implies that the two paths appear as individual channel taps at the receiver only if the system bandwidth is $B_s \geq 400\,\text{MHz}$. If the bandwidth is smaller than that, the paths cannot be resolved in the time domain and will thus appear within the same channel tap at the receiver.

Hence, if we assume that the system bandwidth is not sufficient to temporally resolve the two multi-path components, we can write the sampled channel impulse response, including the effects of transmit/receive filtering, as

$$h[n] \approx \underbrace{\sum_{p=1}^{2} \alpha_p e^{j\varphi_p} g_t(\mathbf{\Psi}_{p,t}) g_r(\mathbf{\Psi}_{p,r})}_{h_0} f[n - n_0]. \tag{4}$$

Here, $f[n]$ denotes the impulse response of the transmit/receive filters and n_0 is the delay in samples of the channel tap in which the two paths appear most significantly. It follows that the relative phase and strength of the two multipath components determines the fading state of the channel tap h_0.

A bandwidth of $400\,\text{MHz}$, as considered in the example above, is not excessively large for state-of-the-art communication systems. Thus, state-of-the-art communication systems may be able to resolve the temporal delay difference $\Delta\tau$ even of closely spaced multi-path components. Yet, most such systems rely on multi-carrier transmission; e.g., 4G/5G utilize orthogonal frequency division multiplexing (OFDM). In such multi-carrier systems, the subcarrier bandwidth is orders of magnitude smaller than the system bandwidth; e.g., 5G new radio employs $120\,\text{kHz}$ in the mmWave band. This implies that even if B_s is sufficiently large to resolve $\Delta\tau$, the channel on each individual subcarrier still appears as frequency-flat, and its fading is determined by the interference of the two paths

$$H[k] \approx \sum_{p=1}^{2} \alpha_p e^{j\varphi_p} g_t(\mathbf{\Psi}_{p,t}) g_r(\mathbf{\Psi}_{p,r}) e^{j\xi_p} F[k]. \tag{5}$$

Here, k denotes the subcarrier index, $F[k]$ is the transfer function corresponding to $f[n]$, and ξ_p is the phase-shift due to the time-delay of the $p-$th channel tap.

C. STOCHASTIC TWO-PATH CHANNEL MODELS

In realistic propagation environments, a purely deterministic two-path channel model as considered above is often too simplistic. Especially in the mmWave domain the phase-difference between the two paths rather has to be modeled as a stochastic random variable, since significant phase variations can be caused by minimal irregularities of the propagation environment; e.g., variations in the electromagnetic scattering/reflection properties of the scattering surfaces or small fluctuations in the propagation distances of the paths due to uneven roadways.

There exists a number of stochastic channel models that are applicable to capture the resulting random variations of the two-path interference pattern: the two-wave (TW) fading model analyzed in [19] describes the fading of two constant amplitude waves with phase-shifts ψ_i that are uniformly distributed in the interval $[0, 2\pi]$

$$h_{\text{TW}} = V_1 e^{j\psi_1} + V_2 e^{j\psi_2}. \tag{6}$$

Here, h_{TW} represents a generic channel coefficient corresponding either to the channel tap h_0 in (4) or to the complex-valued channel gain of subcarrier k in (5). The amplitudes $V_i,\ i \in \{1, 2\}$ and phases ψ_i are determined by the channel parameters α_i, φ_i, $g_t(\mathbf{\Psi}_{i,t})$, $g_r(\mathbf{\Psi}_{i,r})$ and the filter impulse response $f[n]$.

The TWDP model additionally accounts for a so-called diffuse background scattering component that is Rayleigh-distributed $h_d \sim \mathcal{CN}\left(0, 2\sigma_d^2\right)$

$$h_{\text{TWDP}} = V_1 e^{j\psi_1} + V_2 e^{j\psi_2} + h_d. \tag{7}$$

The diffuse scattering component accounts not only for the actual diffuse scattering in the environment, but also for modeling inaccuracies of the two-path model. As described

This article has been accepted for publication in a future issue of this journal, but has not been fully edited. Content may change prior to final publication. Citation information: DOI 10.1109/ACCESS.2020.2981166, IEEE Access

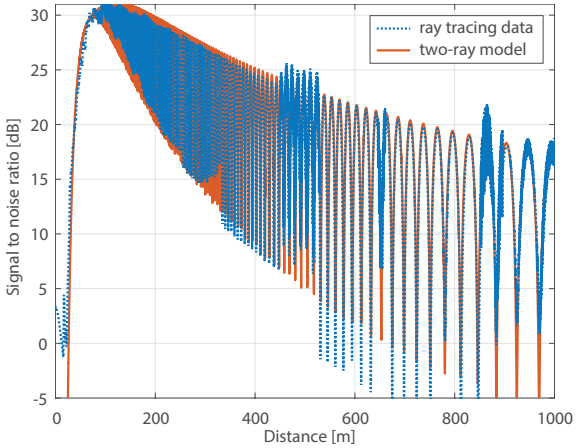

FIGURE 2. Comparison of ray-tracing data of a train-to-infrastructure link with a two-ray channel model according to [16], [30]. The obtained SNR values are valid for a single link without interference.

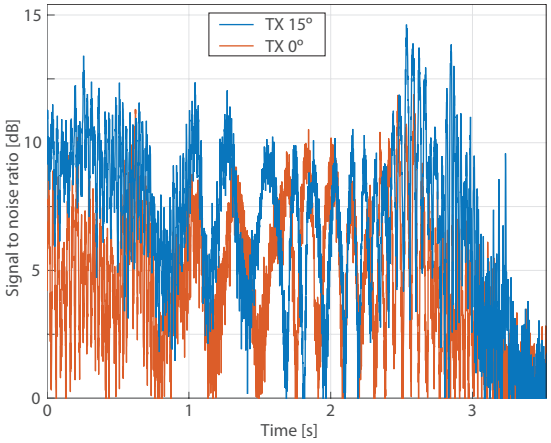

FIGURE 3. Measurement data of an urban car-to-infrastructure link to [18]. The figure shows the measurement traces obtained with two transmit antennas, one pointing towards horizon (TX $0°$) and the other pointing slightly upwards towards the RSU (TX $15°$).

in Section II-D, TWDP fading is well suited to model real-world V2I measurements and ray-tracing channel modeling data.

Further generalizations of the TWDP fading model exist. These generalizations allow for arbitrary probability distributions of the relative phase-shift between the two paths in the generalized two-ray (GTR) fading model [23], as well as, a common random fluctuation of the amplitudes of the two paths, e.g., due to shadowing, in the fluctuating two-ray (FTR) model [24]. The case of more than two specular components with random phases, that is, N-wave with diffuse power fading, is considered in [25]–[27].

D. EVIDENCE FROM MEASUREMENTS AND RAY-TRACING

To justify the two-path model use and discussion above, we include empirical evidence from our prior work from ray-tracing and channel measurements, both in V2I communication scenarios. TW fading for V2X mmWave communications was experimentally observed already decades ago [28], [29]. The more recent results reported here exhibit the even better applicability of TWDP fading.

1) V2I Ray-Tracing Data

The considered ray-tracing setup and data are described in detail in [30]. The authors thereby consider a V2I mmWave railroad communication link at a center frequency of 100 GHz, employing directional antennas with 25 dBi gain on both link ends. The data has subsequently been analyzed in [16]. We show the ray-tracing results of [30, Fig. 7] in Fig. 2 and compare them to the TWDP model proposed in [16]. The TWDP model proposed in [16] follows very accurately the simulated ray-tracing data. The observed fading pattern is dominated by the interference of two paths, except for the regions around 500 m and 850 m, where a third multi-path component slightly distorts the regular two-path interference pattern. The signal to noise ratio (SNR) degradation for small distances is because the receiver is in this region not within the main lobe of the transmit antenna. We can also observe in Fig. 2 that even at 1000 m distance between transmitter and receiver, the considered V2I link has not yet reached the break-point distance, where the pathloss exponent n transitions from free space ($n = 2$) to the asymptotic two-ray ground bounce model ($n = 4$). This break-point distance lies at approximately $d_b \approx \frac{4h_{tx}h_{rx}}{\lambda_c}$, where λ_c is the carrier wavelength [20]. In the considered example, this value equates to $d_b \approx 10$ km implying that the system operates well within the free space propagation regime.

2) V2I Measurement Data

The considered measurement setup and data are described in detail in [18]. The authors thereby consider an urban inner-city mmWave car-to-infrastructure link at a center frequency of 60 GHz. The car is equipped with two horn antennas on the rooftop, which each provide a directional beam with a 3 dB opening angle of $18°$ and a maximum gain of 20 dBi. The first antenna is pointing towards horizon (TX $0°$) and the second antenna is pointing $15°$ upwards towards the RSU (TX $15°$). The RSU is placed on a traffic light at a road intersection mounted at a height of 5 m and is equipped with a monopole antenna with an omnidirectional gain pattern in azimuth. The car is driving towards the RSU with a velocity of 50 km/h. The measurement traces of the SNR achieved with both transmit antennas are shown in Fig. 3. The x-axis represents the measurement time, where the time instant $t = 0$ s corresponds to a transmitter-receiver distance of approximately 40 m and the time instant $t = 3.25$ s corresponds to a position of the car directly below the RSU.

In Fig. 3, we can observe three distinct regions: close to the RSU at around $t = 3$ s, the LOS direction between car and RSU moves out of the main lobe of the antennas and the propagation is therefore dominated by scattering over many multi-path components. Here obviously a two-path fading

model is not applicable, since no dominant direct propagation paths fall within the main lobe of the antennas. Between $t = 0.75\,\mathrm{s}$ and $t = 2.25\,\mathrm{s}$ we mostly observe two-path fading with some diffuse scattering on top. In this region, the LOS between car and RSU lies within the main lobe of the antennas and no other strong scattering objects fall within the main lobe. At larger distances $t < 0.75\,\mathrm{s}$, the car passes close by a truck that is parked next to the street. This truck also falls within the main lobe of the antennas and contributes significantly to the observed fading; therefore, the two-path fading assumption is also not valid in this regime.

Comparing the observations from Figs. 2 and 3, we conclude that the real-world measurement data is more diverse than the ray-tracing data mostly because the scattering environment of the former is more densely populated. The car-to-infrastructure link has been measured in a relatively tight inner-city street canyon with many scatterers (cars and buildings) close by, whereas the considered train-to-infrastructure link is operated in a much more open environment with larger distances to scattering objects. Additionally, the train-to-infrastructure link employs highly directional antennas on both link ends, whereas the car-to-infrastructure link utilizes directional antennas only at the transmitter. For these reasons the two-path fading assumption is better satisfied for the train-to-infrastructure link in our examples.

III. ENHANCING DEPENDABILITY

The observations of the measurement and ray-tracing results above motivate us to investigate the dependability of directional mmWave V2I links under the assumption of TWDP fading. TWDP fading is known to cause a signal outage probability that can be even worse than Rayleigh fading, depending on the relative strength of the two paths [19]. This becomes obvious from Figs. 2 and 3: if the receiver is located at a fading hole of the two-path interference pattern, it can become hard to achieve a minimal required SNR level. Hence, if the communication system has to guarantee dependable connectivity, e.g., to support safety-critical transmissions, diversity has to be exploited to counteract fading effects.

Additionally, the dependability of the V2I communication can be compromised by interference from neighboring transmitters along the road. Even though the pathloss of wireless communication links increases quadratically with the carrier frequency when the antenna gains are assumed constant, interference in directional mmWave V2I communications is still not negligible, since RSUs are commonly placed close to the roads with antennas pointing in LOS along the roads, such that even interference from relatively far away transmitters can have an impact on the intended link quality. As we observed above, the break-point distance d_b in mmWave transmissions is very large, such that often both, intended and interfering signals will experience the same free space propagation pathloss exponent. Thus, some form of transmitter coordination is required to mitigate interference.

A. EXPLOITING DIVERSITY

1) Time and Frequency Diversity

Let us again consider the scenario of Fig. 1 with a direct LOS path and a ground-reflected non line-of-sight (NLOS) path. At larger distances $d_0 \gg h_{tx}, h_{rx}$ the difference in propagation distance between the direct LOS and the ground reflected NLOS path is very well approximated by $\Delta d = |d_{\mathrm{NLOS}} - d_{\mathrm{LOS}}| \approx \frac{2h_{tx}h_{rx}}{d_0}$, and the corresponding phase-difference is $\Delta\varphi = \frac{2\pi}{\lambda_c}\Delta d$. If the receive antenna is located at a fading hole at frequency f_c, how much do we have to change the frequency to get out of the fading hole? To understand this, we calculate the derivative of the phase-difference $\Delta\varphi$ with respect to the frequency at distance d_0

$$\left|\frac{\partial\Delta\varphi}{\partial f}\right|\Bigg|_{f=f_c} \approx \frac{4\pi}{d_0 c_0} h_{tx}h_{rx}. \tag{8}$$

Considering the same railroad communication example as above, with $h_{tx} = 10\,\mathrm{m}$, $h_{rx} = 3.5\,\mathrm{m}$, the phase-derivative equates to $0.85\,^\circ$/MHz at $d_0 = 100\,\mathrm{m}$ and $0.17\,^\circ$/MHz at $d_0 = 500\,\mathrm{m}$. This implies that the fading-state of the channel varies only slowly over frequency and, hence, a relatively large bandwidth is required to achieve substantial frequency diversity. We conclude that for dependable transmission of short messages, which require only a small portion of the bandwidth, it is advisable to employ frequency-hopping to enhance the diversity rather than transmission over a contiguous frequency band.

Similarly, we can calculate the derivative of the phase-difference w.r.t. time. For this purpose, we parametrize the distance as $d = d_0 + v \cdot t$, assuming a constant velocity v. Using the approximation $|d_{\mathrm{NLOS}} - d_{\mathrm{LOS}}| \approx \frac{2h_{tx}h_{rx}}{d_0 + v\cdot t}$, the derivative of the phase difference w.r.t. time is

$$\left|\frac{\partial\Delta\varphi}{\partial t}\right|\Bigg|_{t=0} \approx \frac{4\pi}{d_0^2 c_0} h_{tx}h_{rx}v f_c. \tag{9}$$

With $f_c = 60\,\mathrm{GHz}$ and $v = 100\,\mathrm{km/h}$ and the same heights as above, the phase-derivative w.r.t. time equates to $14\,^\circ$/ms at $d_0 = 100\,\mathrm{m}$ and $0.56\,^\circ$/ms at $d_0 = 500\,\mathrm{m}$. Hence, even though the temporal phase-derivative is orders of magnitude larger than the frequency counterpart, achieving temporal diversity in low-latency sub millisecond communications will not be feasible.[1]

2) Beamforming and Spatial Diversity

The amount of fading (AoF) of a TWDP channel is determined by the relative strength of the two paths: if the two paths are of similar strength, fading holes are very deep, if one path is much stronger than the other, fading holes are shallow. This relative strength of the two paths can be influenced by the beam-pattern of the transmit and/or receive antenna. If the transmitter/receiver is equipped with a steerable phased antenna array, it is possible to minimize the

[1]Notice, this statement does not apply to most car-to-car communication situations, where the distances are commonly a lot smaller and therefore the derivative is larger.

outage probability of the transmission by appropriate beamforming [31]. If the antenna array can form multiple beams, it is even possible to filter-out each path individually and to add them up constructively.[2] However, such beamforming methods are only effective if the two paths can be well separated in the angular domain, which is not likely when the distance d_0 between transmitter and receiver becomes larger.

In such situations, the system has to rely on macroscopic spatial diversity to enhance the dependability. For two-ray fading of a LOS path and a ground-reflected NLOS path as illustrated in Fig. 1, the distance between two fading dips along the propagation direction around distance d_0 is [16]

$$d_f \approx \frac{\lambda_c d_0^2}{2h_{tx}h_{rx}}. \tag{10}$$

Using the same parameters as above, this value equates to $d_f \approx 70\,\text{cm}$ at $d_0 = 100\,\text{m}$ and $d_f \approx 18\,\text{m}$ at $d_0 = 500\,\text{m}$. Hence, with growing transmitter-receiver separation d_0, the distance between antennas has to be fairly large to ensure that diversity can be achieved. Of course, the necessary distance can be reduced by smart placement of the antennas; e.g., an antenna on the left sidewall of a train will likely exhibit an uncorrelated fading state w.r.t. an antenna on the right sidewall. Provided the antennas are placed sufficiently far apart, such that statistically independent channel realizations are obtained, fading of the channel can be counteracted by selection combining or maximum ratio combining (MRC) of the signals from the antennas [32].

In conclusions, achieving diversity in directional communication under TWDP fading is not trivial either in frequency, time or space. The reason for this is that the angular separation between the two dominant paths over such a directional link is small (for larger distances between transmitter and receiver), such that the fading state varies slowly over frequency, time and space. In the context of ultra reliable low latency communication (URLLC), utilizing frequency-hopping with large frequency separation and employing spatial macro-diversity with careful antenna placement is advisable.

B. MITIGATING INTERFERENCE

Interference in mmWave communications is in some publications considered as a minor issue, since the pathloss in the mmWave band is generally so high that interfering signals are only relevant in the case that the interfering beam points directly at the considered user. In V2I communications, however, this situation is not unlikely to occur, as the antenna beams of RSUs all point along the same straight road, as illustrated in Fig. 1. This implies that the LOS direction to the intended and interfering transmitters can be very similar and, as mentioned above, since the break-point distance d_b in the mmWave band is very large, the signal to interference ratio (SIR) can then be low. In such situations, some form of interference mitigation will be required to enhance the dependability of the communication link.

If the receiver is equipped with multiple antennas, we mentioned above that fading of the intended signal can be counteracted by MRC. However, applying the MRC weights of the intended signal to the interference can increase the fading of the interference and, thus, cause a net negative effect on the signal to interference and noise ratio (SINR) statistics. We will observe such effects in Section IV, where we numerically investigate a railroad communications example. Hence, if interference is present, the applied receive filter should be interference-aware to improve the dependability; e.g., an interference-aware minimum mean squared error (MMSE) filter. This, of course, requires estimation of the interference channels.

At the transmitter-side well-known coordinated multi-point (CoMP) transmission techniques can be employed for interference mitigation [33]–[35]. Notice, though, that coordinated beamforming may not be effective in a situation as illustrated in Fig. 1, as the directions of the intended and interfering signals are too similar and thus beamforming cannot distinguish between them. Then, the system will have to resort to the less resource efficient coordinated scheduling [36]. Of course, even better performance can be achieved by joint transmission CoMP, which, however, may be hard to realize in the considered high-mobility V2I scenarios, due to its restrictive requirements regarding channel state information available at the transmitter (CSIT) [37], [38].

IV. RAILROAD COMMUNICATIONS EXAMPLE

In this section, we investigate a railroad communication scenario under the assumptions of Rice and TWDP fading. We evaluate the ergodic performance of the system, in terms of average SINR and ergodic capacity, as well as, its outage performance. We start by investigating a single transmitter scenario without interference in Section IV-B, and afterwards assess the impact of interference in a multiple transmitter scenario in Section IV-C.

The considered scenario is illustrated in Fig. 1: a railroad is served by a number of base stations that are equally spaced along the railroad with distance $d_{tx} = 1000\,\text{m}$ in-between. Each base station is equipped with a directional antenna that achieves a 3 dB beam-width of $10°$, a maximum gain of 25 dBi and a side-lobe-suppression ratio of 25 dB. The antennas are placed at heights $h_{tx} = 10\,\text{m}$ and $h_{rx} = 3\,\text{m}$. We assume that the beamforming directions of the base stations are fixed. Specifically, each base station points a beam to the center of the stretch of railroad that is served by the base station; i.e., the beam points towards the ground at 250 m distance from the base station. The train itself is equipped with antennas that have the same parameters as the base station antennas. However, we assume that the antennas on the train are steerable, such that they always point directly along the LOS between train and serving base station. We consider one or more antennas equally spaced on the coach of length $\ell_c = 25\,\text{m}$. When multiple receive antennas are

[2] A similar approach can of course also be applied in the time domain, provided the bandwidth is sufficiently large to resolve the individual paths.

This article has been accepted for publication in a future issue of this journal, but has not been fully edited. Content may change prior to final publication. Citation information: DOI 10.1109/ACCESS.2020.2981166, IEEE Access

used, we assume that the antennas are positioned on the coach in such a way that statistically independent channel realizations are obtained; in terms of the achievable diversity, this corresponds to a best-case scenario. Finally, we assume that the system operates at a bandwidth of $B_s = 1\,\text{GHz}$ and a carrier frequency of $f_c = 100\,\text{GHz}$ following the ray-tracing setup of [30].

A. CHANNEL MODELING

Motivated by the considerations in Sec. II, we model the channel between each directional transmit and receive antenna either via Rice fading or via TWDP fading. Rice fading can be considered as a best-case benchmark, which occurs whenever only the LOS is present. The Rice assumption is often employed for directional communication links. However, as we have seen above, it is generally too optimistic. To determine the average receive powers of the intended and interfering signals, we employ a frequency and distance dependent pathloss model. As the break-point distance for the considered scenario is large $d_b \approx 10\,\text{km}$, we employ a free space pathloss exponent of $n = 2$.

Both, TWDP fading and Rice fading are characterized by a K-factor, which quantifies the relative strength of the specular components and the diffuse component. According to the model derived in [16], the K-factor for the considered scenario is set equal to $30\,\text{dB}$. Additionally, for TWDP fading, we have to calculate the relative strength of the two specular components. This relative strength is quantified by the so-called Δ-parameter [19]; utilizing the notation of Eq. (7) we have $\Delta = 2V_1V_2/(V_1^2 + V_2^2)$. Notice, TWDP fading reduces to Rice fading when $\Delta = 0$. As recognized in [16], the Δ-parameter for the considered scenario can be given in closed-form and is determined by the antenna gain pattern, the angles of the LOS and NLOS directions, and the scattering properties of the ground. In our considered scenario, the Δ-parameter increases with growing distance between transmitter and receiver, implying that the relative strength of the two specular components becomes more and more similar. This is intuitive, since with growing distance the angle of the LOS and the NLOS ground reflection, and thus the antenna gain exhibited by both paths, become increasingly similar. A detailed explanation of the channel modeling approach is provided in [16].

B. SINGLE TRANSMITTER – INTERFERENCE-FREE TRANSMISSION

In our first numerical example, we consider a single active base station along the railroad, i.e., an interference-free transmission. We investigate the probability distribution of the SNR and its impact on the achievable transmission rate and the dependability of the communication link.

1) Single Receive Beam

If the train is equipped with a single antenna that forms a single receive beam along the LOS, the fading distribution of the SNR at the receiver is solely determined by the fading of the channel gain. For the case that the channel gain follows a TWDP distribution, a semi-closed-form of the probability density function (pdf) of the SNR, as well as, results on the ergodic capacity and the average symbol error probability are provided in [23].[3] Furthermore, the outage probability, i.e., the probability that the achievable rate, or equivalently the SNR, falls below a prescribed threshold can be evaluated by a single one-dimensional integral.

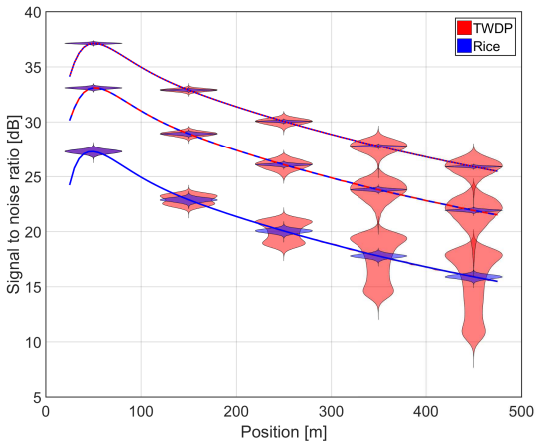

FIGURE 4. Signal to noise ratio considering Rice/TWDP fading and MRC with $N_r = 1$ (solid bottommost curves), $N_r = 4$ (dashed middle curves) and $N_r = 10$ (dotted topmost curves) when no interferers are present.

In Fig. 4, we show simulation results of the mean SNR as a function of the position d_0 of the train. The bottommost solid lines correspond to the case of a single receive antenna $N_r = 1$. The blue curves are obtained with Rice fading and the red curves with TWDP fading. The parameters of both fading distributions are set such that the mean SNRs of both distributions coincide. In addition to the mean values, we also illustrate the pdf of the SNR at selected positions $d_0 \in \{50, 150, 250, 350, 450\}\,\text{m}$ by means of violin plots. We observe that close to the base station, TWDP fading exhibits the same distribution as Rice fading, implying that the Δ-parameter is close to zero. This is because in this case the angle between the LOS and the ground reflected NLOS path is large, such that the NLOS path experiences a much smaller antenna gain than the LOS. Far away from the base station, we observe the converse situation: the angle between the LOS and NLOS paths is very similar, such that both arrive at the receiver with practically the same strength, leading to deep fading holes.

In Table 1, we summarize the simulation results at position $d_0 = 475\,\text{m}$, corresponding to the worst-case position in terms of fading and mean SNR. The first row $N_r = 1$ of the table *Performance without Interference* is relevant for the current simulations. The first two columns represent ergodic values, namely the ergodic capacity and the mean SINR. These values are relevant if the block-length of the forward error correction code (FEC) of the system is long enough to

[3] Notice, the GTR-U model proposed in [23] is the same as TWDP.

This article has been accepted for publication in a future issue of this journal, but has not been fully edited. Content may change prior to final publication. Citation information: DOI 10.1109/ACCESS.2020.2981166, IEEE Access

	capacity [bits/s/Hz]		mean SINR [dB]		fading margin [dB]		robust SINR [dB]		robust rate [bits/s/Hz]	
	Rice	TWDP	Rice	TWDP	Rice	TWDP	Rice	TWDP	Rice	TWDP
Performance without Interference										
$N_r = 1$	5.2	4.9	15.5	15.5	0.6	6.7	14.9	8.8	5.0	3.1
$N_r = 4$	7.2	7.1	21.5	21.5	0.3	5.1	21.2	16.4	7.1	5.5
$N_r = 10$	8.5	8.5	25.5	25.5	0.2	2.9	25.3	22.6	8.4	7.5
Performance with Interference										
$N_r = 1$	3.0	3.1	8.5	10.2	0.8	10.6	7.7	-0.4	2.8	0.9
$N_r = 4$	5.2	5.1	16.4	16.4	7.1	10.4	9.3	6.0	3.3	2.3
$N_r = 10$	6.5	6.5	20.5	20.5	8.9	9.7	11.6	10.8	3.9	3.7

TABLE 1. Summary of simulation results at position $d_0 = 475$ m with MRC receiver. The fading margin w.r.t. the mean SINR is chosen such as to achieve an outage probability of 10^{-3}.

effectively cover all fading states of the channel. We observe that Rice and TWDP fading perform very similar in terms of ergodic values.

For low-latency short-message communication, i.e., URLLC, the outage probability of the system is a more relevant performance metric than the ergodic capacity, since coding over many fading states is not possible. Here, Rice and TWDP fading exhibit very different behavior. In the table, we provide the necessary fading margin w.r.t. the mean SINR to achieve an outage probability of 10^{-3}. Additionally, we provide the corresponding robust SINR values and transmission rates for which the system has to be dimensioned in order to achieve this outage probability. We observe that for Rice fading with a K-factor of 30 dB, the fading margin is very small and, thus, the ergodic values are very similar to the robust values. For TWDP fading, however, a very large fading margin is required as the Δ-parameter is close to one; correspondingly, the robust SINR and rate are far below the mean SINR and the ergodic capacity, respectively.

2) Spatial Receive Diversity

If the train is equipped with multiple spatially distributed antennas, we can apply selection combining or MRC of the signals to reduce the fading of the channel. This is shown by the middle and the topmost curves in Fig. 4. With multiple antennas, not only the mean SNR improves, but additionally the AoF reduces. This is reflected by the ergodic and robust SINR and rate values provided in Table 1 *Performance without Interference*. With $N_r = 10$ the robust rate of the TWDP channels can be more than doubled compared to $N_r = 1$, as the required fading margin with $N_r = 10$ is a lot smaller. A theoretical performance analysis of MRC over identically distributed TWDP fading channels is available in [39]. For the case of non-identical TWDP fading channels, to the best of our knowledge, theoretical performance results are only available for dual-branch MRC [40]; hence, a general performance analysis of MRC over an arbitrary number of non-identical TWDP channels is still an open problem.

C. MULTIPLE TRANSMITTERS – INTERFERENCE-AFFLICTED TRANSMISSION

In our second simulation example, we consider all other base stations shown in Fig. 1 as interferers for the intended base station. In Table 1 *Performance with Interference*, we summarize the corresponding results. Considering the case with $N_r = 1$, we observe that surprisingly the mean SINR of TWDP fading is better than that of Rice fading, even though the mean power of the intended signal is the same. This, however, hardly translates to a gain in terms of ergodic capacity. Even worse, the required fading margin of the TWDP channel increases significantly compared to the *Performance without Interference*, causing a significant net reduction of the robust transmission rate. Notice that, to the best of our knowledge, the theoretical performance of transmission over TWDP channels under TWDP interference has not yet been analyzed in literature. We have derived some initial results on the outage probability of this situation in [41]; however, this analysis requires numerical calculations and is hardly feasible for larger number of base stations.

If we increase the number of antennas and apply MRC of the intended signal, we again achieve a gain in terms of the mean SINR. The required fading margin for TWDP fading, however, hardly reduces with growing N_r; for Rice fading, the fading margin even grows substantially with growing N_r. The reason for this is that, even though MRC reduces the AoF of the intended signal, it increases the AoF of the interference and thereby also the variations of the SINR. For example, a random combination of two Rice-distributed interfering signals results in TWDP fading of the effective interference, thus increasing the AoF of the SINR. This can be observed in the empirical cumulative distribution functions (ecdfs) of the SINR shown in Fig. 5: with a single receive antenna, Rice fading exhibits almost a deterministic SINR behavior, whereas with growing N_r the distribution of the SINR broad-

This article has been accepted for publication in a future issue of this journal, but has not been fully edited. Content may change prior to final publication. Citation information: DOI 10.1109/ACCESS.2020.2981166, IEEE Access

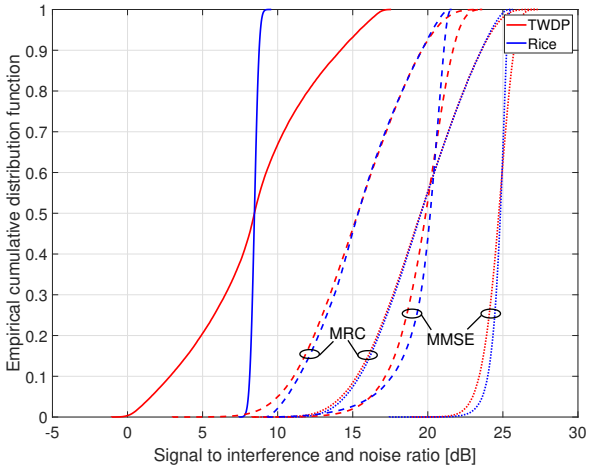

FIGURE 5. ECDF of the SINR at $d_0 = 475$ m considering Rice/TWDP fading and MRC/MMSE with $N_r = 1$ (solid), $N_r = 4$ (dashed) and $N_r = 10$ (dotted) when interferers are present.

ens due to variations of the effective interference. To the best of our knowledge, no theoretical results on this effect are available in the literature nor is the distribution of the SINR known analytically. Combining the two effects of improving mean SINR and increasing required fading margin, we still obtain a net improvement in terms of robust SINR and robust rate with growing N_r; however, compared to the ergodic values, the improvement of the robust values is modest for the Rice fading situation.

A remedy to this problem is to apply an interference-aware MMSE receiver. This receiver can achieve both: interference suppression, and thus reduction of the AoF due to interference, plus reduction of the AoF of the intended signal. In Fig. 5, we provide a comparsion of the ecdf of the SINR achieved by the MRC and MMSE receivers for Rice and TWDP fading channels. We observe that the interference-aware MMSE receiver achieves better mean SINR, as well as, reduced AoF compared to MRC. Especially if the number of antennas is larger than the number of interferers, the AoF can be significantly reduced.

Notice, in our simulation scenario of Fig. 1, most of the interference is caused by the neighboring base station on the left of the intended base station, even though the interferer on the right is closer to the train. The reason for this is that the LOS direction of the interferer on the left is very similar to the intended signal and therefore it lies within the main lobe of the receive antenna on the train. If we apply coordinated scheduling between the intended base station and this single strongest interferer, most of the interference can be eliminated and the performance is very similar to the interference-free scenario [42]. However, this may not be feasible in a practical situation with several parallel railroad tracks and trains. Alternatively, it might be helpful to place base stations further off the track, such that trains can be distinguished in their azimuthal LOS direction, thus allowing for coordinated beamforming in the azimuth domain.

V. CONCLUSION

In this article, we discussed the applicability of two-ray channel models for directional mmWave V2I communication scenarios. We reviewed V2I measurement results, as well as, ray-tracing data from literature, which both exhibit a distinct two-path interference pattern. We argued that the directional antennas at the transmitter and/or receiver act as spatial filters that effectively limit the richness of the multipath channel to two dominant paths, a direct LOS path and a ground reflected NLOS path. Since in the mmWave domain the phase-difference, and thus the interference condition, of these two paths is sensitive to variations in the propagation geometry, we argued that TWDP fading is well suited to model directional mmWave V2I communication scenarios. Based on these insights, we then investigated the ergodic performance of latency-unconstrained large block-length transmissions, as well as, the required fading margin to support dependable low-latency short block-length communications. Even though the ergodic performance of TWDP fading turned out to be very similar to Rice fading in our simulations, its outage behavior was much worse. We showed that enhancing the dependability of the transmission by exploiting diversity is not easy to achieve, as the fading state of the channel varies slowly especially over frequency, but also over time and space. The situation becomes even more intricate when interferers are present, since a reduction in the amount of fading of the intended signal power by exploiting diversity may even increase the fading of the SINR due to the interference. In conclusion, when TWDP fading is present in directional mmWave V2I communications, a significant amount of diversity, as well as, sophisticated interference mitigation strategies are required to support dependable wireless connectivity.

REFERENCES

[1] S. S. Husain, A. Kunz, A. Prasad, E. Pateromichelakis, and K. Samdanis, "Ultra-high reliable 5G V2X communications," IEEE Communications Standards Magazine, vol. 3, no. 2, pp. 46–52, June 2019.

[2] F. Tang, Y. Kawamoto, N. Kato, and J. Liu, "Future intelligent and secure vehicular network toward 6G: Machine-learning approaches," Proceedings of the IEEE, vol. 108, no. 2, pp. 292–307, Feb 2020.

[3] J. Moreno, J. M. Riera, L. d. Haro, and C. Rodriguez, "A survey on future railway radio communications services: challenges and opportunities," IEEE Communications Magazine, vol. 53, no. 10, pp. 62–68, Oct 2015.

[4] S. Schwarz, T. Philosof, and M. Rupp, "Signal processing challenges in cellular assisted vehicular communications," IEEE Signal Processing Magazine, vol. 34, no. 2, pp. 47–59, March 2017.

[5] R. Mendez-Rial, C. Rusu, N. Gonzalez-Prelcic, A. Alkhateeb, and R. W. Heath, "Hybrid MIMO architectures for millimeter wave communications: Phase shifters or switches?" IEEE Access, vol. 4, pp. 247–267, January 2016.

[6] H. Ji, Y. Kim, J. Lee, E. Onggosanusi, Y. Nam, J. Zhang, B. Lee, and B. Shim, "Overview of full-dimension MIMO in LTE-advanced pro," IEEE Communications Magazine, vol. 55, no. 2, pp. 176–184, February 2017.

[7] C. Mecklenbräuker, A. Molisch, J. Karedal, F. Tufvesson, A. Paier, L. Bernado, T. Zemen, O. Klemp, and N. Czink, "Vehicular channel characterization and its implications for wireless system design and performance," Proceedings of the IEEE, vol. 99, no. 7, pp. 1189–1212, July 2011.

[8] R. He, O. Renaudin, V. Kolmonen, K. Haneda, Z. Zhong, B. Ai, and C. Oestges, "A dynamic wideband directional channel model for vehicle-to-vehicle communications," IEEE Transactions on Industrial Electronics, vol. 62, no. 12, pp. 7870–7882, Dec 2015.

[9] B. Antonescu, M. T. Moayyed, and S. Basagni, "mmWave channel propagation modeling for V2X communication systems," in IEEE 28th Annual International Symposium on Personal, Indoor, and Mobile Radio Communications (PIMRC), pp. 1–6, Oct 2017.

[10] S. Jaeckel, L. Raschkowski, K. Börner, and L. Thiele, "Quadriga: A 3-D multi-cell channel model with time evolution for enabling virtual field trials," IEEE Transactions on Antennas and Propagation, vol. 62, no. 6, pp. 3242–3256, June 2014.

[11] F. Ademaj, S. Schwarz, T. Berisha, and M. Rupp, "A spatial consistency model for geometry-based stochastic channels," IEEE Access, vol. 7, pp. 183 414–183 427, 2019.

[12] 3GPP, "TSG RAN; study on 3D channel model for LTE (release 12)," http://www.3gpp.org/DynaReport/36873.htm, Dec. 2017.

[13] 3GPP, "TSG RAN; study on channel model for frequencies from 0.5 to 100 GHz," http://www.3gpp.org/DynaReport/38901.htm, Dec. 2019.

[14] J. Lee, J. Choi, J. Lee, and S. Kim, "28 GHz millimeter-wave channel models in urban microcell environment using three-dimensional ray tracing," IEEE Antennas and Wireless Propagation Letters, vol. 17, no. 3, pp. 426–429, March 2018.

[15] S. Hussain and C. Brennan, "Efficient preprocessed ray tracing for 5g mobile transmitter scenarios in urban microcellular environments," IEEE Transactions on Antennas and Propagation, vol. 67, no. 5, pp. 3323–3333, May 2019.

[16] E. Zöchmann, J. Blumenstein, R. Marsalek, M. Rupp, and K. Guan, "Parsimonious channel models for millimeter wave railway communications," in IEEE Wireless Communications and Networking Conference (WCNC), pp. 1–6, 2019.

[17] E. Zöchmann, M. Hofer, M. Lerch, S. Pratschner, L. Bernadó, J. Blumenstein, S. Caban, S. Sangodoyin, H. Groll, T. Zemen, A. Prokes, M. Rupp, A. Molisch, and C. Mecklenbräuker, "Position-specific statistics of 60 GHz vehicular channels during overtaking," IEEE Access, vol. 2019, no. 7, pp. 14 216–14 232, 2019.

[18] H. Groll, E. Zöchmann, S. Pratschner, M. Lerch, D. Schützenhöfer, M. Hofer, J. Blumenstein, S. Sangodoyin, T. Zemen, A. Prokes, et al., "Sparsity in the delay-Doppler domain for measured 60 GHz vehicle-to-infrastructure communication channels," in IEEE International Conference on Communications Workshops (ICC Workshops), pp. 1–6. IEEE, 2019.

[19] G. D. Durgin, T. S. Rappaport, and D. A. de Wolf, "New analytical models and probability density functions for fading in wireless communications," IEEE Transactions on Communications, vol. 50, no. 6, pp. 1005–1015, Jun 2002.

[20] T. S. Rappaport, Y. Xing, G. R. MacCartney, A. F. Molisch, E. Mellios, and J. Zhang, "Overview of millimeter wave communications for fifth-generation (5G) wireless networks—with a focus on propagation models," IEEE Transactions on Antennas and Propagation, vol. 65, no. 12, pp. 6213–6230, Dec 2017.

[21] P. Almers, E. Bonek, A. Burr, N. Czink, M. Debbah, V. Degli-Esposti, H. Hofstetter, P. Kyösti, D. Laurenson, G. Matz, A. Molisch, C. Oestges, and H. Özcelik, "Survey of channel and radio propagation models for wireless MIMO systems," EURASIP Journal on Wireless Communications and Networking, vol. 2007, no. 019070, pp. 1–19, 2007.

[22] V. Va, J. Choi, and R. W. Heath, "The impact of beamwidth on temporal channel variation in vehicular channels and its implications," IEEE Transactions on Vehicular Technology, vol. 66, no. 6, pp. 5014–5029, June 2017.

[23] M. Rao, F. J. Lopez-Martinez, M. S. Alouini, and A. Goldsmith, "MGF approach to the analysis of generalized two-ray fading models," IEEE Transactions on Wireless Communications, vol. 14, no. 5, pp. 2548–2561, May 2015.

[24] J. M. Romero-Jerez, F. J. Lopez-Martinez, J. F. Paris, and A. J. Goldsmith, "The fluctuating two-ray fading model: Statistical characterization and performance analysis," IEEE Transactions on Wireless Communications, vol. 16, no. 7, pp. 4420–4432, July 2017.

[25] S. Schwarz, "Outage investigation of beamforming over random-phase finite-scatterer MISO channels," IEEE Signal Processing Letters, vol. 24, no. 7, pp. 1029–1033, July 2017.

[26] Y. J. Chun, "A generalized fading model with multiple specular components," 2018.

[27] J. M. Romero-Jerez, F. J. Lopez-Martinez, J. P. Peña-Martin, and A. Abdi, "Stochastic fading channel models with multiple dominant specular components for 5G and beyond," 2019.

[28] H. Meinel and A. Plattner, "Millimetre-wave propagation along railway lines," IEE Proceedings F (Communications, Radar and Signal Processing), vol. 130, no. 7, pp. 688–694, 1983.

[29] A. Kato, K. Sato, M. Fujise, and S. Kawakami, "Propagation characteristics of 60-GHz millimeter waves for ITS inter-vehicle communications," IEICE Transactions on Communications, vol. 84, no. 9, pp. 2530–2539, 2001.

[30] K. Guan, G. Li, T. Kürner, A. F. Molisch, B. Peng, R. He, B. Hui, J. Kim, and Z. Zhong, "On millimeter wave and THz mobile radio channel for smart rail mobility," IEEE Transactions on Vehicular Technology, vol. 66, no. 7, pp. 5658–5674, July 2017.

[31] S. Schwarz, "Signal outage optimized beamforming for MISO TWDP fading channels," in IEEE International Symposium on Personal, Indoor and Mobile Radio Communications, pp. 1–6, Bologna, Italy, Sept. 2018.

[32] S. Schwarz and E. Zöchmann, "Robust beam-alignment for TWDP fading millimeter wave channels," in IEEE 20th International Workshop on Signal Processing Advances in Wireless Communications (SPAWC), pp. 1–5, July 2019.

[33] L. Zhu, F. R. Yu, B. Ning, and T. Tang, "Design and performance enhancements in communication-based train control systems with coordinated multipoint transmission and reception," IEEE Transactions on Intelligent Transportation Systems, vol. 15, no. 3, pp. 1258–1272, June 2014.

[34] S. Schwarz and M. Rupp, "Exploring coordinated multipoint beamforming strategies for 5G cellular," IEEE Access, vol. 2, pp. 930–946, 2014.

[35] J. Zhang, Y. Ji, S. Jia, H. Li, X. Yu, and X. Wang, "Reconfigurable optical mobile fronthaul networks for coordinated multipoint transmission and reception in 5G," IEEE/OSA Journal of Optical Communications and Networking, vol. 9, no. 6, pp. 489–497, June 2017.

[36] M. Li, I. B. Collings, S. V. Hanly, C. Liu, and P. Whiting, "Multicell coordinated scheduling with multiuser zero-forcing beamforming," IEEE Transactions on Wireless Communications, vol. 15, no. 2, pp. 827–842, Feb 2016.

[37] S. Schwarz and M. Rupp, "Evaluation of distributed multi-user MIMO-OFDM with limited feedback," IEEE Transactions on Wireless Communications, vol. 13, no. 11, pp. 6081–6094, Aug. 2014.

[38] T. R. Lakshmana, A. Tölli, and T. Svensson, "Improved local precoder design for JT-CoMP with periodical backhaul CSI exchange," IEEE Communications Letters, vol. 20, no. 3, pp. 566–569, March 2016.

[39] R. Subadar and A. D. Singh, "Performance of M-MRC receivers over TWDP fading channels," AEU - International Journal of Electronics and Communications, vol. 68, no. 6, pp. 569 – 572, 2014.

[40] A. Dinamani Singh and R. Subadar, "Performance of dual MRC over non-identical TWDP fading channels," in International Conference on Advances in Computer Engineering and Applications, pp. 88–92, March 2015.

[41] S. Schwarz, "Outage-based admission control for multi-user MISO transmission with imperfect CSIT," in IEEE 86th Vehicular Technology Conference, pp. 1–5, Toronto, Canada, Sept. 2017.

[42] M. K. Müller, M. Taranetz, and M. Rupp, "Providing current and future cellular services to high speed trains," IEEE Communications Magazine, vol. 53, no. 10, pp. 96–101, October 2015.

STEFAN SCHWARZ received his PhD in telecommunications engineering from Technical University of Vienna (TU Wien), Austria, in 2013. He currently holds a tenure track position as Assistant Professor at the Institute of Telecommunications, TU Wien. His research interests are in wireless communications, signal processing and channel modeling. Address: Gußhausstraße 25, Institute of Telecommunications, 1040 Vienna, Austria. Email: sschwarz@nt.tuwien.ac.at

ERICH ZÖCHMANN received his PhD in telecommunications engineering from Technical University of Vienna (TU Wien), Austria, in 2019. He is currently employed as a research engineer at PIDSO Propagation Ideas and Solutions GmbH. His research interests are in millimeter wave communications, channel modeling and wireless signal propagation. Address: Wallackgasse 2, 1230 Vienna, Austria. Email: ezoechma@nt.tuwien.ac.at

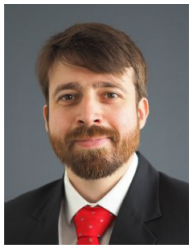

MARTIN MÜLLER received his PhD in telecommunications engineering from Technical University of Vienna (TU Wien), Austria, in 2018. He currently holds a post-doc position as Project Assistant at the Institute of Telecommunications, TU Wien. His research interests are in system level simulations, mobile communications and stochastic geometric modeling of wireless networks. Address: Gußhausstraße 25, Institute of Telecommunications, 1040 Vienna, Austria. Email: mmueller@nt.tuwien.ac.at

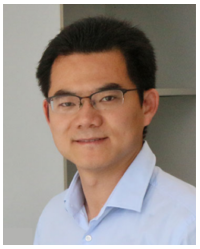

KE GUAN received his PhD in information and telecommunication systems from Beijing Jiaotong University, China, in 2014. He is an Associate Professor at Beijing Jiatong University and a Humboldt Research Fellow of the Technical University of Braunschweig, Germany. His research interests are in railroad communications, millimeter wave and THz transmissions, and channel modeling. Address: State Key Lab of Rail Traffic Control and Safety, Siyuan Building, Beijing Jiatong University, 100044 Beijing, China. Email: kguan@bjtu.edu.cn